Nonlinear Dyn (2016) 86:535–541
DOI 10.1007/s11071-016-2906-y

ORIGINAL PAPER

Nonlinear dynamics of a generalized higher-order nonlinear Schrödinger equation with a periodic external perturbation

Min Li · Lei Wang · Feng-Hua Qi

Received: 8 March 2016 / Accepted: 14 June 2016 / Published online: 28 June 2016
© Springer Science+Business Media Dordrecht 2016

Abstract The nonlinear dynamics of a generalized higher-order nonlinear Schrödinger (HNLS) equation with a periodic external perturbation is investigated numerically. Via the phase plane analysis, we find that both the homoclinic orbits and heteroclinic orbits can exist for the unperturbed HNLS equation under certain conditions, which respectively corresponds to the bell-shaped and kink-shaped soliton solutions. Moreover, under the effect of the periodic external perturbation, the quasi-periodic bifurcations arise and can evolve into the chaos. The dynamical responses of the perturbed system varying with the perturbation strength and two types of chaotic attractors are discussed to show the existence of the chaotic motions. Via the feedback control methods, such chaotic motions are found to be controlled effectively and finally evolve into the stable quasi-periodic orbits. All the results are helpful to understand the dynamical properties of the nonlinear system.

Keywords Generalized higher-order nonlinear Schrödinger equation · Periodic external perturbation · Homoclinic orbits · Heteroclinic orbits · Chaos control

M. Li (✉) · L. Wang
Department of Mathematics and Physics, North China Electric Power University, Beijing 102206, China
e-mail: micheller85@126.com

F.-H. Qi
School of Information, Beijing Wuzi University, Beijing 101149, China

1 Introduction

In recent years, nonlinear behaviors of the soliton equations under the external perturbations have been paid much attentions, since there often exist various perturbations in real physical systems [1–12]. For instance, the perturbations arising in Korteweg–de Vries (KdV) equation can be used to describe the resonant forcing in a tank of finite length [1], traveling steady pressure distribution on the water of finite depth [2] and solitons generated by moving pressure disturbances [3]; the perturbed sine-Gordon equation was used to model the propagations of nonlinear waves through the quasi-periodic or chaotic media [5]. Studies show that the addition of the perturbation to an integrable equation can lead to the chaotic dynamics, which is a type of interesting nonlinear phenomenon [6–8,10]. The chaotic motions in plasma physics have been found through the perturbed nonlinear Schrödinger equation (NLS) when a uniform plasma is driven by an external rf field [6,7]. By a period-doubling sequence, a route to chaos has been investigated in a perturbed sine-Gordon system [8,9]. The existence of the chaotic behaviors for the KdV equation with the external Hamiltonian perturbations has been studied by the Melnikov theory [10].

As a special partial differential equation, the perturbed NLS equation has been proposed and can exhibit the observable chaotic behavior in the time domain [11,12], which was given as follows:

$$iu_t = u_{xx} + 2|u|^2u + i\varepsilon\left[\widehat{D}u + \Gamma e^{2i\Omega^2 t}\right], \qquad (1)$$

where $u = u(x,t)$ is an even and periodic function with the period $L = 2\pi$ in the spatial variable x, Γ is the real forcing amplitude, $2\Omega^2$ denotes the real frequency, $\widehat{D}$ is a bounded and negative operator, and $\varepsilon \geq 0$ is a small parameter. By means of the simple linear damping term $\widehat{D}u \equiv -\alpha\, u$, Bishop et al first observed numerically the peculiar jumping of solutions around the plane waves of Eq. (1), which has been found to be connected with the homoclinic solutions in the unperturbed limit [12,13]. Besides, Ref. [11] has proved the existence of a complicated and self-similar family of homoclinic bifurcations.

Those previous studies of the perturbed NLS equation mainly considered the simple linear damping term in the perturbation $\widehat{D}u$. When $\Gamma = 0$, Eq. (1) can be used to describe the slowly varying electromagnetic waves in optical fibers [14,27,28]. However, for the ultrashort pulses propagation in the high-bit-rate and long-distance communication, some higher-order linear and nonlinear terms have to be incorporated into the NLS equation [14]. In this paper, we focus on the following generalized higher-order NLS (HNLS) equation with a periodic external perturbation:

$$\begin{aligned} & i\, q_z + \alpha_1 q_{tt} + \alpha_2 |q|^2 q \\ & \quad + i\,\varepsilon \left[\alpha_3 q_{ttt} + \alpha_4 |q|^2 q_t + \alpha_5 q \left(|q|^2\right)_t\right] \\ & \quad = i\,\varepsilon\,\omega\, e^{-i\,\chi^2 t}, \end{aligned} \tag{2}$$

where $q = q(z,t)$ is the slowly varying envelope of the electric field, z and t are the normalized distances along the direction of the propagation and retarded time, ε denotes the ratio of the width of the spectra to the carrier frequency, α_1, α_2, α_3, α_4 and α_5 are all real parameters related to the effects of group velocity dispersion, self-phase modulation, third-order dispersion, self-steepening and stimulated Raman scattering in optical fibers, respectively [15]. The frequency χ^2 is a real number, and ω is an arbitrary constant. When $\omega = 0$, Eq. (2) reduces to a generalized higher-order NLS equation, which is integrable and can describe the phenomenon of ultrashort pulses properly [16,17]. The bright and dark soliton solutions under certain conditions have been obtained by the inverse scattering transform, Darboux transformation and Hirota method [18–22].

Hereby, the dynamic behaviors of Eq. (2) will be analyzed to find that whether the periodic external perturbation can lead to the chaos and how to control it. Phase plane analysis will be performed for the unperturbed equation and the case with the periodic perturbation, respectively, in Sect. 2. During the process, we will analyze the existence of the homoclinic orbits and heteroclinic orbits for the unperturbed system, and the possibility of the transition from the quasi-periodic bifurcations to the chaotic motions under the effect of the periodic perturbation. In Sect. 3, we will use the bifurcation diagrams, maximum Lyapunov exponents and phase portraits to further investigate the chaotic behaviors of Eq. (2). Moreover, we will try to control the chaos of Eq. (2) by means of two methods. Section 4 will be our conclusions.

2 Phase plane analysis

By introducing the traveling wave transformation,

$$q(z,t) = \phi(\xi) e^{i\,\Theta} \tag{3}$$

with

$$\xi = a(t - c\,z), \quad \Theta = K\,t - \Omega\,z, \tag{4}$$

we transform Eq. (2) into the following form

$$\beta_1\,\phi'' + \beta_2\,\phi + \beta_3\,\phi^3 - \varepsilon\omega \sin\left(\frac{K}{a}\,\xi\right) = 0 \tag{5}$$

with

$$\chi^2 = \Omega - c\,z, \quad K = \frac{\alpha_1}{4\varepsilon\,\alpha_3}, \quad \alpha_1 = \frac{6\alpha_2\alpha_3}{2\alpha_4 + \alpha_5},$$

$$\Omega = -K\left(c - 3K\alpha_1 + 4K^2\varepsilon\alpha_3\right),$$

$$\beta_1 = \frac{3a^2\varepsilon\alpha_2\alpha_3}{4\varepsilon\alpha_4 + 2\varepsilon\alpha_5}, \quad \beta_3 = \frac{\varepsilon\alpha_2\,(\alpha_4 + 2\alpha_5)}{4\varepsilon\alpha_4 + 2\varepsilon\alpha_5},$$

$$\beta_2 = \frac{3\alpha_2\left[45\alpha_2^2\alpha_3 + 4c\varepsilon\,(2\alpha_4 + \alpha_5)^2\right]}{8\varepsilon^2(2\alpha_4 + \alpha_5)^3},$$

where a, c, K and Ω are the constants and the prime means the differentiation with respect to the new variable ξ. Such system is different from the general nonlinear Duffing oscillator equation, which usually includes the dissipation or damping term [23,24]. The parameters β_1, β_2 and β_3 determine whether the fluctuations are chaotic or regular. In the next parts, we analyze the fixed points and phase orbits of System (5). As we know, dynamical behaviors of phase orbits near the equilibrium points can reflect the types of solutions for the ordinary differential equation [25,26]. Usually, for the nonlinear partial differential equations (NPDEs)

with complex dependent variables [e.g., Eq. (2)], homoclinic and heteroclinic orbits of the nonlinear ordinary differential equations derived from the NPDEs indicate the existence of the bright and dark soliton solutions [26].

2.1 Unperturbed system

For the unperturbed case of System (5), we have

$$\beta_1 \phi'' + \beta_2 \phi + \beta_3 \phi^3 = 0, \tag{6}$$

which is equivalent to the two-dimensional (2D) plane autonomous system as follows ($X \equiv \phi$, $Y \equiv \phi_\xi$):

$$X' = Y, \quad Y' = -\frac{\beta_2}{\beta_1} X - \frac{\beta_3}{\beta_1} X^3. \tag{7}$$

This system is an integrable Hamiltonian system with the Hamiltonian function

$$H(X, Y) = \frac{1}{2} Y^2 + \frac{\beta_2}{2\beta_1} X^2 + \frac{\beta_3}{4\beta_1} X^4. \tag{8}$$

The fixed points and their stability of System (7) are given in the following:

(1) For $\beta_2/\beta_3 \geqslant 0$, there is only one fixed point $(0, 0)$: $(0, 0)$ is a center if $\beta_2/\beta_1 > 0$, while $(0, 0)$ is an unstable saddle point if $\beta_2/\beta_1 < 0$.

(2) For $\beta_2/\beta_3 < 0$, System (7) possesses three equilibrium points: S_0 [$(0, 0)$], S_1 [$(\sqrt{-\beta_2/\beta_3}, 0)$] and S_2 [$(-\sqrt{-\beta_2/\beta_3}, 0)$]. If $\beta_2/\beta_1 < 0$, S_0 is an unstable saddle point, while both S_1 and S_2 are the centers, which means that there exist the homoclinic orbits to S_0 enclosing the centers S_1 and S_2. If $\beta_2/\beta_1 > 0$, S_0 is a center, while both S_1 and S_2 are the unstable saddle points, which indicates that the phase orbits behave in the heteroclinic form.

The analysis above shows that Eq. (2) with $\omega = 0$ admits the bell-shaped soliton solutions if $\beta_2/\beta_3 < 0$ and $\beta_2/\beta_1 < 0$, while the kink-shaped soliton solutions arise if $\beta_2/\beta_3 < 0$ and $\beta_2/\beta_1 > 0$.

2.2 Perturbed system

With the periodic perturbations considered, the closed homoclinic or heteroclinic orbits will break. In this part, we analyze the phase orbits of System (5) and show the homoclinic or heteroclinic chaotic motions.

Equation (5) is equivalent to a 3D plane autonomous system as follows ($X \equiv \phi$, $Y \equiv \phi_\xi$, $Z \equiv \frac{K}{a}\xi$):

$$\begin{aligned} X' &= Y, \quad Z' = \frac{K}{a}, \\ Y' &= -\frac{\beta_2}{\beta_1} X - \frac{\beta_3}{\beta_1} X^3 + \frac{\varepsilon\omega}{\beta_1} \sin(Z). \end{aligned} \tag{9}$$

Such system can be seen as the coupling of two motion systems: One is the nonlinear system (i.e., $\varepsilon = 0$), and the other one is the linear harmonic oscillation system caused by the external periodic perturbation.

Since the conditions for the unperturbed System (7) to possess the homoclinic or heteroclinic orbits are given in Sect. 2.1, we will discuss the effect of periodic perturbation on those two types of orbits by choosing the parameters properly. Hereby, the small perturbation parameter is chosen as $\varepsilon = 0.1$. With the parameters in System (10) satisfying the conditions $\beta_2/\beta_3 < 0$ and $\beta_2/\beta_1 < 0$, the phase portraits of the homoclinic orbits and bifurcations can be seen in Fig. 1. The single-period homoclinic orbits enclosing the centers $(-3/\sqrt{5}, 0)$ and $(3/\sqrt{5}, 0)$ can be seen in Fig. 1a by choosing $\omega = 0$. When $\omega > 0$, the closed period orbits break which leads to the quasi-periodic bifurcations. When the strength of periodic perturbation is quite small, the oscillation of the linear system is week and System (10) exhibits the quasi-periodic motions around one center of the nonlinear system, as seen in Fig. 1b. If we increase the value of ω to obtain the large periodic perturbation, such system will have the transition oscillations around two centers and the chaotic motions will arise, as seen in Fig. 1c.

Similarly, if we choose the parameters in System (10) under the conditions $\beta_2/\beta_3 < 0$ and $\beta_2/\beta_1 > 0$, we can obtain the phase portraits of the heteroclinic orbits and bifurcations in Fig. 2. The single-periodic heteroclinic orbits across three points can be seen in Fig. 2a. Similarly, the quasi-periodic bifurcation occurs when we consider the effect of periodic perturbation, i.e., $\omega = 0.2$, as seen in Fig. 2b. If the value of the parameter ω is further increased, the quasi-periodic bifurcation changes into the chaotic motion, which can be seen in Fig. 2c.

Based on the above analysis of the phase portraits, it is found that the increase in the strength of the periodic perturbation can lead to the transfer from the quasi-periodic bifurcations to the chaotic motions for System (10).

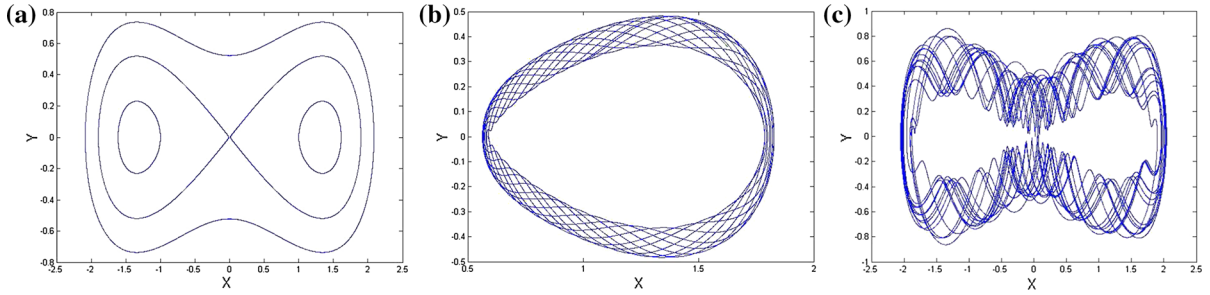

Fig. 1 Phase portraits of System (2): **a** Homoclinic orbits across five points $(0.01, 0)$, $(-0.01, 0)$, $(-1, 0)$, $(1, 0)$ and $(1, -0.7)$ with $\beta_1 = 3/10$, $\beta_2 = -0.09$, $\beta_3 = 0.05$, $\omega = 0$, $K = 3$, $a = 1$ and $\varepsilon = 0.1$; **b** quasi-periodic motion with the parameters chosen the same as those in **a** except $\omega = 0.5$; **c** chaotic motion, where the parameters are chosen the same as those in **a** except $\omega = 2$

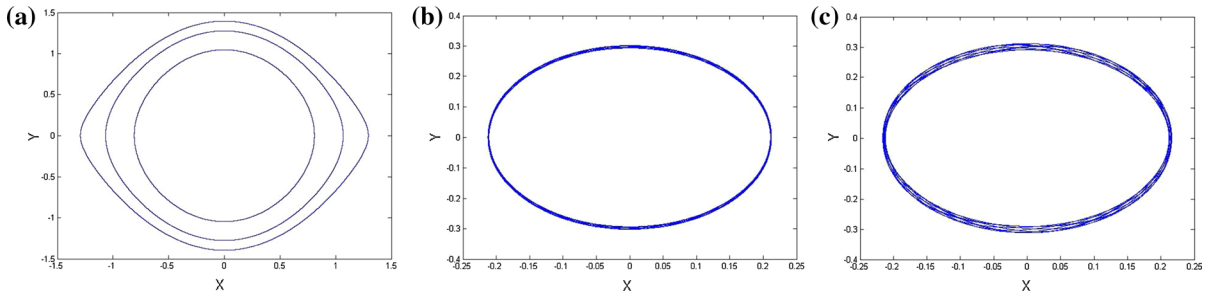

Fig. 2 Phase portraits of System (2): **a** Heteroclinic orbits across there points $(1, 0.4)$, $(0.5, 0.8)$ and $(1, 0.707)$ with $\beta_1 = 1$, $\beta_2 = 2$, $\beta_3 = -1$, $\omega = 0$, $K = 5$, $a = 1$ and $\varepsilon = 0.1$; **b** weak chaotic motion across the point $(0.2, 0.1)$ with $\omega = 0.2$ and other parameters are chosen the same as those in **a**; **c** strong chaotic motion across the point $(0.2, 0.1)$ with $\omega = 2$ and other parameters are chosen the same as those in **a**

3 Chaos analysis and control of Eq. (2)

In this part, we investigate the bifurcation and chaotic motions of Eq. (2) which are the interesting nonlinear phenomena and have great applications in many fields such as the technological, engineering, telecommunications, ecology [27,28]. The addition of a perturbation can lead to the system non-integrable. So, the analysis is proceeded around the plane wave solution of Eq. (2). According to the analysis on the phase portraits of the perturbed System (5), there exist two types of chaos which are stimulated by the homoclinic and heteroclinic bifurcations, respectively. Therefore, we will discuss those two cases in the following.

By fixing the parameters $\beta_1 = 3/10$, $\beta_2 = -0.09$, $\beta_3 = 0.05$, $K = 3$, $a = 1$ and $\varepsilon = 0.1$ in System (10) and taking the perturbation strength ω as a bifurcation parameter, we obtain the dynamical response of such system varying with ω in (ω, X) plane, as shown in Fig. 3a. It is found that the chaotic motions only arise in the positive direction of X-axis when ω is chosen less than about 1, while the chaotic motions will arise in both direction of X-axis if the value of ω is greater than 1. Such bifurcation diagram is in agree with the analysis on the phase orbits in Fig. 1b, c. The corresponding largest Lyapunov exponents and the chaotic attractor at $\omega = 2$ are given in Fig. 3b, c, which confirm the existence of chaotic motions.

For the case of heteroclinic bifurcation, we choose $\beta_1 = 1$, $\beta_2 = 2$, $\beta_3 = -1$, $K = 5$, $a = 1$ and $\varepsilon = 0.1$ such that $\beta_2/\beta_3 < 0$ and $\beta_2/\beta_1 > 0$. The corresponding bifurcation diagram in (ω, X) plane and the maximum Lyapunov exponent are given in Fig. 4a, b, respectively, which indicate the existence of the chaotic motion from $\omega = 0$. Moreover, the chaotic attractor of Fig. 4a at $\omega = 2$ can be seen in Fig. 4c.

In order to inhibit and eliminate the chaotic motions of Eq. (2) under the effect of the periodic external per-

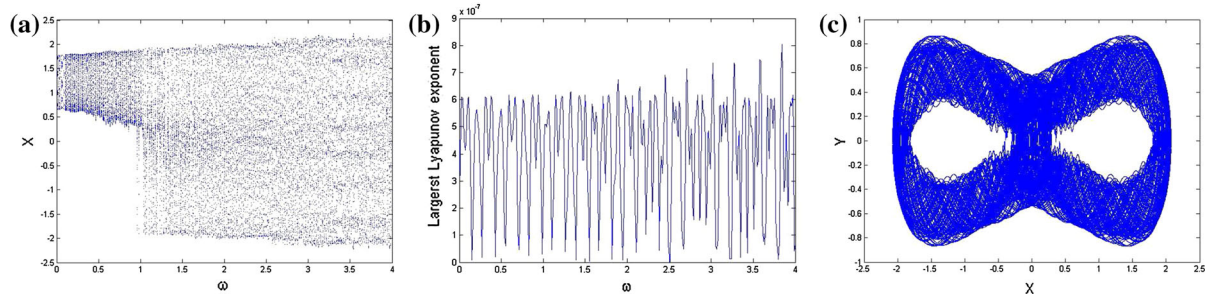

Fig. 3 **a** Homoclinic bifurcation diagram of System (5) in (ω, X) plane with $\beta_1 = 3/10$, $\beta_2 = -0.09$, $\beta_3 = 0.05$, $K = 3$, $a = 1$ and $\varepsilon = 0.1$; **b** maximum Lyapunov exponent of **a**; **c** chaotic attractor of **a** at $\omega = 2$

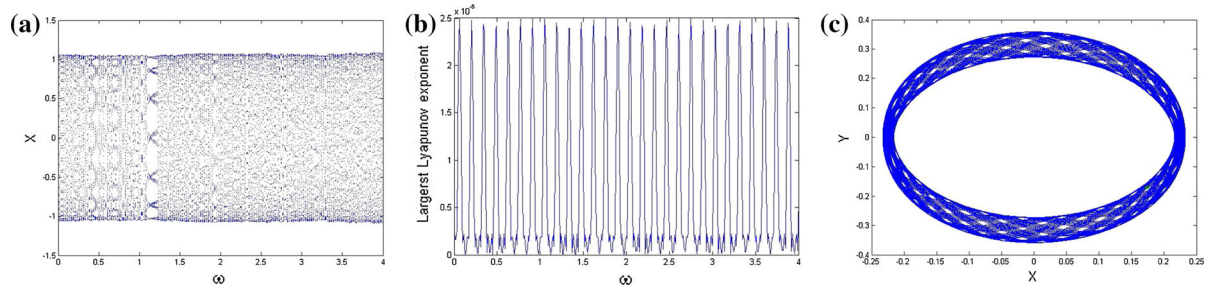

Fig. 4 **a** Heteroclinic bifurcation diagram of System (5) in (ω, X) plane with $\beta_1 = 1$, $\beta_2 = 2$, $\beta_3 = -1$, $K = 5$, $a = 1$ and $\varepsilon = 0.1$; **b** maximum Lyapunov exponent of **a**; **c** chaotic attractor of **a** at $\omega = 2$

turbation, we will control the chaos by choosing effective methods.

First of all, the variable feedback control method [29] is applied to control the chaos of Case I. In this method, a small parameter is introduced to stabilize the chaotic orbits of the initial system and form new nonchaotic orbits. Moreover, the change in such small parameter has little influence on the system and can keep the initial dynamical behaviors. When a feedback variable is added into System (10) reduced from Eq. (2), the controllable system can be obtained as follows:

$$\begin{aligned} X' &= Y - \eta X, \quad Z' = \frac{K}{a}, \\ Y' &= -\frac{\beta_2}{\beta_1} X - \frac{\beta_3}{\beta_1} X^3 + \frac{\varepsilon\omega}{\beta_1} \sin(Z), \end{aligned} \tag{10}$$

where η is an adjustable feedback coefficient. The small change in the feedback coefficient can also weaken the chaotic behavior obviously. Therefore, the chaos of System (10) can be suppressed by choosing the proper value of η. For the first case, as seen from Fig. 3a, System (10) with $\eta = 0$ is chaotic when the parameters are chosen as $\beta_1 = 3/10$, $\beta_2 = -0.09$, $\beta_3 = 0.05$, $K = 3$, $\omega = 2$, $a = 1$ and $\varepsilon = 0.1$. The global bifurcation of System (10) with respect to the feedback coefficient η is shown in Fig. 5a. We can find that the quasi-periodic windows arise when $\eta > 0$. Moreover, System (10) will evolve into the stable quasi-periodic orbits as the value of η increases. In order to show such phenomenon clearly, Fig. 5b, c is plotted to give the phase portraits of system at $\omega = 0.025$ and $\omega = 0.07$, respectively. Therefore, by means of the variable feedback control method, System (10) reduced from Eq. (2) can be controlled well.

Further, we apply the coupled feedback control method [30] to find that whether the chaos stimulated by the heteroclinic bifurcations can be inhibited effectively. The idea of such method is to use the coupling of the periodic signal $Y(t)$ and the output result of System (5) $X(t)$ ($\phi \equiv X(t)$) as the control signal $f(t)$, that is, $f(t) = L[X(t) - Y(t)]$, where L denotes the strength of the control signal. Then, System (10) reduced from Eq. (2) can be modified into the controllable form:

$$\begin{aligned} X' &= Y, \quad Z' = \frac{K}{a}, \\ Y' &= -\frac{\beta_2}{\beta_1} X - \frac{\beta_3}{\beta_1} X^3 + \frac{\varepsilon\omega}{\beta_1} \sin(Z) + L(X - Y). \end{aligned} \tag{11}$$

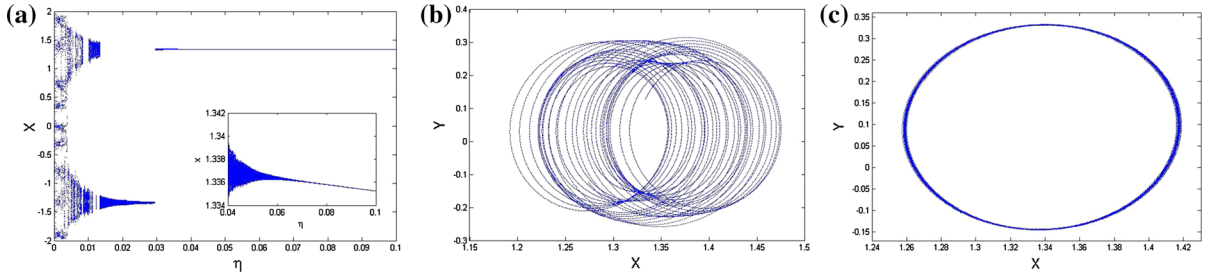

Fig. 5 **a** Global bifurcation diagram of System (10) in (η, X) plane with $\beta_1 = 3/10$, $\beta_2 = -0.09$, $\beta_3 = 0.05$, $K = 3$, $\omega = 2$, $a = 1$ and $\varepsilon = 0.1$; **b** phase portrait of **a** at $\eta = 0.025$; **c** phase portrait of **a** at $\eta = 0.07$

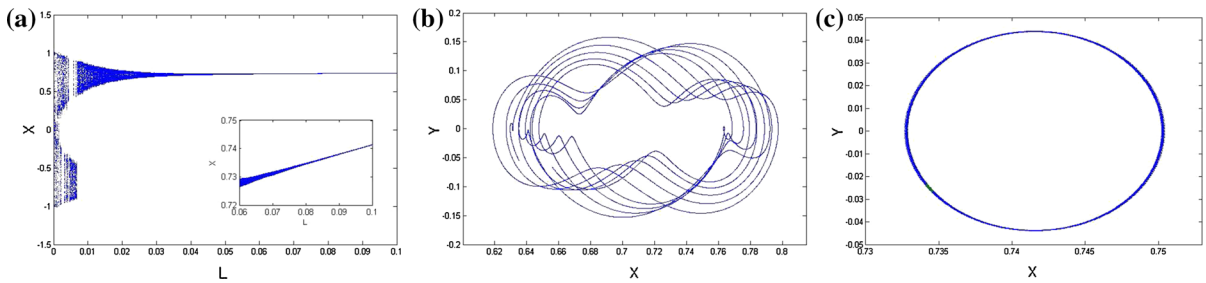

Fig. 6 **a** Global bifurcation diagram of System (11) in (L, X) plane with $\beta_1 = 1$, $\beta_2 = 2$, $\beta_3 = -1$, $K = 5$, $a = 1$ and $\varepsilon = 0.1$; **b** phase portrait of **a** at $L = 0.02$; **c** phase portrait of **a** at $L = 0.1$

Similarly, Fig. 6a is the global bifurcation of System (11) with respect to the feedback coefficient L for $0 \leqslant L \leqslant 0.1$. It is found that such system can evolve into the quasi-periodic orbits from the chaos as the value of L increases. With the fixed feedback coefficients, the phase portraits of System (11) at $L = 0.02$ and $L = 0.1$ are shown in Fig. 6b, c, respectively, which further indicate that System (10) reduced from Eq. (2) can also be controlled well by use of the coupled feedback control method.

4 Conclusions

The nonlinear dynamics of a generalized HNLS equation with a periodic external perturbation [i.e., Eq. (2)] has been investigated numerically. Phase plane analysis has been performed for the unperturbed equation and the case with the periodic perturbation, respectively. The homoclinic orbits and heteroclinic orbits are found to be existent for the unperturbed system (7), which indicates that Eq. (2) with $\omega = 0$ possesses the bell-shaped and kink-shaped soliton solutions. Based the analysis on the effects of the periodic perturbation, we have found that the increase in the strength of the periodic perturbation can lead to the transition from the quasi-periodic bifurcations to the chaotic motions. Moreover, the dynamical responses of the perturbed system (10) varying with the perturbation strength and two types of chaotic attractors have been discussed, which shows the existence of the chaotic motions of Eq. (2). By means of the feedback control methods, those two types of chaotic motions are found to be controlled effectively and can evolve into the stable quasi-periodic orbits. Those results are important for understanding the dynamical properties of Eq. (2).

Acknowledgments This work has been supported by the Fundamental Research Funds of the Central Universities (Project Nos. 2014QN30, 2014ZZD10 and 2015ZD16), by the National Natural Science Foundations of China (Grant Nos. 61505054, 11426105, 11305060 and 11371371), by the Postdoctoral Science Foundation of China (2014T70061) and by the Higher-Level Item Cultivation Project of Beijing Wuzi University (No. GJB20141001).

References

1. Cox, E.A., Mortell, M.P.: The evolution of resonant water-wave oscillations. J. Fluid Mech. **162**, 99–116 (1986)

2. Wu, T.Y.: Generation of upstream advancing solitons by moving disturbances. J. Fluid Mech. **184**, 75–99 (1987)
3. Akylas, T.R.: On the excitation of long nonlinear water waves by a moving pressure distribution. J. Fluid Mech. **141**, 455–466 (1984)
4. Zhuang, K.G., Du, Z.J., Lin, X.J.: Solitary waves solutions of singularly perturbed higher-order KdV equation via geometric singular perturbation method. Nonlinear Dyn. **80**, 629–635 (2015)
5. Charles Li, Y.: Homoclinic tubes and chaos in perturbed. Chaos Solitons Fractals **20**, 791–798 (2004)
6. Morales, G.J., Lee, Y.C.: Ponderomotive-force effects in a nonuniform plasma. Phys. Rev. Lett. **33**, 1016 (1974)
7. Moon, H.T.: Homoclinic crossings and pattern selection. Phys. Rev. Lett. **64**, 412 (1990)
8. Zheng, D.J., Yeh, W.J., Symko, O.G.: Period doubling in a perturbed sine-Gordon system, a long Josephson junction. Phys. Lett. A **140**, 225–228 (1989)
9. Bishop, A.R., Flesch, R., Forest, M.G., McLaughlin, D.W., Overman, E.A.: Correlations between chaos in a perturbed sine-Gordon equation and a truncated model system. SIAM J. Math. Anal. **21**, 1511–1536 (1990)
10. Blyuss, K.B.: Chaotic behaviour of nonlinear waves and solitons of perturbed Korteweg–de Vries equation. Rep. Math. Phys. **46**, 47–54 (2000)
11. Haller, G.: Homoclinic jumping in the perturbed nonlinear Schrödinger equation. Commun. Pure Appl. Math. **52**, 1–47 (1999)
12. Bishop, A.R., Forest, M.G., McLaughlin, D.W., Overman, E.A.: A modal representation of chaotic attractors for the driven, damped pendulum chain. Phys. Lett. A **144**, 17–25 (1990)
13. Haller, G., Wiggins, S.: Multi-pulse jumping orbits and homoclinic trees in a modal truncation of the damped-forced nonlinear Schrödinger equation. Phys. D **85**, 311–347 (1995)
14. Agrawal, G.P.: Nonlinear Fiber Optics. Academic, California (2002)
15. Porsezian, K.: Soliton models in resonant and nonresonant optical fibers. Pramāna **57**, 1003–1039 (2001)
16. Hirota, R.: Exact envelope-soliton solutions of a nonlinear wave equation. J. Math. Phys. **14**, 805–809 (1973)
17. Sasa, N., Satsuma, J.: New-type of soliton solutions for a higher-order nonlinear Schrödinger equation. J. Phys. Soc. Jpn. **60**, 409–417 (1991)
18. Xu, Z.Y., Li, L., Li, Z.H., Zhou, G.S.: Soliton interaction under the influence of higher-order effects. Opt. Commun. **210**, 375–384 (2002)
19. Gilson, C., Hietarinta, J., Nimmo, J., Ohta, Y.: Sasa–Satsuma higher-order nonlinear Schrödinger equation and its bilinearization and multisoliton solutions. Phys. Rev. E **68**, 016614 (2008)
20. Palacios, S.L., Guinea, A., Fernández, J.M., Crespo, R.D.: Dark solitary waves in the nonlinear Schrödinger equation with third order dispersion, self-steepening, and self-frequency shift. Phys. Rev. E **60**, R45–R47 (1999)
21. Jiang, Y., Tian, B., Li, M., Wang, P.: Bright hump solitons for the higher-order nonlinear Schröinger equation in optical fibers. Nonlinear Dyn. **74**, 1053–1063 (2013)
22. Xu, J., Fan, E.: The unified transform method for the Sasa–Satsuma equation on the half-line. Proc. R. Soc. A **469**, 20130068 (2013)
23. Korsch, H.J., Jodl, H.J., Hartmann, T.: Chaos. Springer, Berlin (2008)
24. Georgiev, Z.D.: Analysis and synthesis of oscillator systems described by perturbed single well Duffing equations. Nonlinear Dyn. **62**, 883–893 (2010)
25. Liu, S.D., Liu, S.K.: Soliton Wave and Turbulence. (Chinese version) Shanghai, Shanghai Scientific and Technological Education (1994)
26. Infeld, E., Rowlands, G.: Nonlinear Waves, Solitons and Chaos. Cambridge Univ, Cambridge (2000)
27. Biswas, A., Song, M., Zerrad, E.: Bifurcation analysis and implicit solution of Klein-Gordon equation with dual-power law nonlinearity in relativistic quantum mechanics. Int. J. Nonlinear Sci. Numer. Simul. **14**, 317 (2013)
28. Song, M., Liu, Z.R., Biswas, A.: Soliton solution and bifurcation analysis of the KP-Benjamin-Bona-Mahoney equation with power law nonlinearity. Nonlinear Anal. Model. Control **20**, 417 (2015)
29. Kakmeni, F., Bowong, S., Tchawoua, C., Kaptouom, E.: Strange attractors and chaos control in a Duffing–van der Pol oscillator with two external periodic forces. J. Sound Vib. **227**, 783–799 (2004)
30. Shi, Y.X., Bai, D.Y., Tao, W.J.: Chaos and control of the Duffing–van der Pole equation with two external periodic excitations. J. Hebei Normal Univ. **34**, 631–635 (2010)